Two different Approaches for Evaluating Dynamic Reactivity for Predictor-Corrector Quasi-Static Monte-Carlo Simulation

Taesuk Oh [a], Inyup Kim [a], and Yonghee Kim [a*]
[a] *Nuclear and Quantum Engineering, Korea Advanced Institute of Science and Technology (KAIST), 291 Daehak-ro, Yuseong-gu, Daejeon 34141, Republic of Korea*
[*] *Corresponding author: yongheekim@kaist.ac.kr*

1. Introduction

Recently, the Monte Carlo (MC) based transient reactor analysis is gaining attention in both practical and academic senses with drastic improvement in the high-power computing resources. There are two-different approaches mainly being recognized for time-dependent MC calculation, which are namely the Dynamic Monte Carlo (DMC) and the Predictor-Corrector Quasi-Static Monte Carlo (PCQS-MC) methods. Both methods have been successfully implemented and validated in several MC codes, e.g., the DMC approach for TRIPOLI-4 [1], McCARD [2], Serpent2 [3], OpenMC [4], and PCQS-MC approach for McBOX [5], RMC [6]. The iMC code, which is a continuous energy MC code recently developed in KAIST, supports both methods based on the user's preference [7].

Unlike the conventional steady-state MC calculation, the evaluation of uncertainty is rather complicated for both transient methods. To circumvent such an issue for the PCQS-MC calculation, the PK-sampling method has been proposed and adapted to the iMC code, where reasonable uncertainty estimation comparable to the real variance is possible [8].

It should be noted that the calculation of dynamic reactivity is necessary for performing the PCQS-MC calculation, where two different approaches can be envisioned, i.e., the difference in the calculation scheme for dynamic reactivity concerning RMC and iMC. With the aid of the PK-sampling capacity supported by the iMC code, a comparison is made in terms of both the accuracy and uncertainty of the two approaches applied for the TWIGL benchmark problem.

2. Predictor-Corrector Quasi-Static Monte Carlo

2.1 Transient Fixed Source Problem (TFSP)

To describe the transient behaviour of the reactor system, the following set of equations must be solved:

$$\frac{1}{v(E)}\frac{\partial\psi(\vec{r},E,\vec{\Omega},t)}{\partial t} = -L\psi(\vec{r},E,\vec{\Omega},t) - T\psi(\vec{r},E,\vec{\Omega},t) + S\psi(\vec{r},E,\vec{\Omega},t) + \sum_{d=1}^{G_d}\frac{\chi_d(E)}{4\pi}\lambda_d C_d(\vec{r},t) + \frac{1}{k_0}\frac{\chi_p(E)}{4\pi}(1-\beta)F\psi(\vec{r},E,\vec{\Omega},t), \quad (1)$$

$$\frac{\partial C_d(\vec{r},t)}{\partial t} = \frac{1}{k_0}\beta_d F\psi(\vec{r},E,\vec{\Omega},t) - \lambda_d C_d(\vec{r},t), \quad (2)$$

where L, T, S, and F represent the leakage, transport, scattering, and fission operators respectively, and all the other notations are that of the convention.

With implementation of implicit Euler method, linear variation of fission source term, and exponential transformation, one garners the following transient fixed source problem (TFSP).

$$\begin{aligned}&\left(L+\tilde{T}_{PCQS}-S\right)\psi(\vec{r},E,\vec{\Omega},t_s)\\ &=\frac{\psi(\vec{r},E,\vec{\Omega},t_{s-1})e^{\gamma_s\Delta t}}{v(E)\Delta t_s}+\sum_{d=1}^{G_d}\frac{\chi_d(E)}{4\pi}\lambda_d C_d(\vec{r},t_{s-1})f_{1,d}\\ &+\sum_{d=1}^{G_d}\frac{\chi_d(E)}{4\pi}\frac{\beta_d F\psi(\vec{r},E,\vec{\Omega},t_{s-1})}{k_0}f_{2,d}\\ &+\sum_{d=1}^{G_d}\frac{\chi_d(E)}{4\pi}\frac{\beta_d F\psi(\vec{r},E,\vec{\Omega},t_s)}{k_0}f_{3,d}\\ &+\frac{1}{k_0}\frac{\chi_p(E)}{4\pi}(1-\beta)F\psi(\vec{r},E,\vec{\Omega},t_s)=S_{PCQS}(\vec{r},E,\vec{\Omega},t_s),\end{aligned} \quad (3)$$

where

$$\begin{aligned}&\tilde{T}_{PCQS}\psi(\vec{r},E,\vec{\Omega},t_s)\\ &=\left(\sigma_t(\vec{r},E,t_s)+\frac{1}{v(E)\Delta t_s}+\frac{\gamma_s}{v(E)}\right)\psi(\vec{r},E,\vec{\Omega},t_s).\end{aligned} \quad (4)$$

2.2 Point-Kinetics Equation

Whilst updating the angular flux according to Eq. (3), the point-kinetics (PK) parameters is tallied. Note that it is the calculation of PK equation that finally determines the power of the reactor system during transient. For the formulation of the PK equation, the angular flux is factorized into the amplitude function n(t) and the shape function as:

$$\psi(\vec{r},E,\vec{\Omega},t) = n(t)\,\varphi(\vec{r},E,\vec{\Omega},t), \quad (5)$$

with an additional equation to render such a factorization to be unique.

$$\begin{aligned}&\int dV\int d\vec{\Omega}\int dE\; W(\vec{r},E,\vec{\Omega})\frac{\varphi(\vec{r},E,\vec{\Omega},t)}{v(E)}\\ &=\int dV\int d\vec{\Omega}\int dE\; W(\vec{r},E,\vec{\Omega})\frac{\psi(\vec{r},E,\vec{\Omega},t_0)}{v(E)},\end{aligned} \quad (6)$$

where $W(\vec{r},E,\vec{\Omega})$ denotes a weighting function. Substituting Eqs. (5) and (6) into Eqs (1) and (2), the PK equation can be acquired.

$$\frac{dn(t)}{dt} = \left(\frac{\rho(t) - \beta(t)}{\Lambda(t)} \right) n(t) + \sum_{d=1}^{G_d} \lambda_d c_d(t),$$
$$\frac{dc_d(t)}{dt} = -\lambda_d c_d(t) + \frac{\beta_d(t)}{\Lambda(t)} n(t). \quad (7)$$

The associated notations are defined as below:

- Dynamic Reactivity $\rho(t)$

$$\rho(t) = 1 - \frac{k_0}{k(t)} \quad (8)$$

$$k(t) = \frac{\left\langle W(\vec{r},E,\vec{\Omega}), \frac{\chi(E)}{4\pi} F\varphi(\vec{r},E,\vec{\Omega},t) \right\rangle}{\left\langle W(\vec{r},E,\vec{\Omega}), (L+T-S)\varphi(\vec{r},E,\vec{\Omega},t) \right\rangle} \quad (9)$$

- Delayed Neutron Fraction $\beta(t)$

$$\beta(t) = \sum_{d=1}^{G_d} \beta_d(t) \quad (10)$$

$$\beta_d(t) = \frac{\left\langle W(\vec{r},E,\vec{\Omega}), \frac{\chi_d(E)}{4\pi} \beta_d F\varphi(\vec{r},E,\vec{\Omega},t) \right\rangle}{\left\langle W(\vec{r},E,\vec{\Omega}), \frac{\chi(E)}{4\pi} F\varphi(\vec{r},E,\vec{\Omega},t) \right\rangle} \quad (11)$$

- Generation time $\Lambda(t)$

$$\Lambda(t) = \frac{\left\langle W(\vec{r},E,\vec{\Omega}), \frac{1}{v(E)} \varphi(\vec{r},E,\vec{\Omega},t) \right\rangle}{\left\langle W(\vec{r},E,\vec{\Omega}), \frac{1}{k_0} \frac{\chi(E)}{4\pi} F\varphi(\vec{r},E,\vec{\Omega},t) \right\rangle} \quad (12)$$

- Precursor Concentration $c_d(t)$

$$c_d(t) = \frac{\left\langle W(\vec{r},E,\vec{\Omega}), \frac{\chi_d(E)}{4\pi} C_d(\vec{r},t) \right\rangle}{\left\langle W(\vec{r},E,\vec{\Omega}), \frac{1}{v(E)} \varphi(\vec{r},E,\vec{\Omega},t) \right\rangle} \quad (13)$$

where bracket denotes the integration over the whole phase space. Note that a unit vector has been generally considered for the weighing function in this work, i.e., $W(\vec{r},E,\vec{\Omega}) \rightarrow 1.0$.

2.3 Tallying Dynamic Reactivity

As aforementioned, there are two different approaches for tallying Eqs. (8) and (9). The multiplication factor k_0 in Eq. (8) is the eigenvalue obtained for the steady-state calculation. Hence, it is the determination of $k(t)$ that dictates the dynamic reactivity. The numerator for Eq. (9) can be easily estimated by multiplying $\nu\sigma_f$ whilst tracking a particle during the transport process.

The constituent elements in the denominator for Eq. (9) can be directly tallied. The transport (T) and the scattering (S) terms can be estimated as

$$< (T-S)\psi(\vec{r},E,\vec{\Omega},t) > = < \sigma_a(\vec{r},E,t)\psi(\vec{r},E,\vec{\Omega},t) >, \quad (14)$$

and the leakage term (L) can be calculated by scoring the number (or weights) of particles egressing out of the reactor system.

$$< L\psi(\vec{r},E,\vec{\Omega},t) > = < \vec{\Omega} \cdot \nabla \psi(\vec{r},E,\vec{\Omega},t) > = \int dE \oint d\vec{S} \cdot \int d\vec{\Omega}\, \vec{\Omega}\, \psi(\vec{r},E,\vec{\Omega},t). \quad (15)$$

On the contrary, one could assess the denominator of Eq. (9) indirectly, which is the method applied in the RMC code [9]. The net source term S_{PCQS} in Eq. (3) is updated for every active cycle. Considering the overall balance between the source and loss terms, it is obvious that the following relation holds:

$$\begin{aligned} &< S_{PCQS}(\vec{r},E,\vec{\Omega},t_s) > \\ &= < \left(L + \tilde{T}_{PCQS} - S \right) \psi(\vec{r},E,\vec{\Omega},t_s) > \\ &= < \left(L + T - S \right) \psi(\vec{r},E,\vec{\Omega},t_s) > \\ &+ < \left(\frac{1}{v(E)\Delta t} + \frac{\gamma_s}{v(E)} \right) \psi(\vec{r},E,\vec{\Omega},t_s) > \end{aligned} \quad (16)$$

By re-arranging the necessary terms, one yields:

$$\begin{aligned} &< \left(L + T - S \right) \psi(\vec{r},E,\vec{\Omega},t_s) > \\ &= < S_{PCQS}(\vec{r},E,\vec{\Omega},t_s) > \\ &- < \left(\frac{1}{v(E)\Delta t} + \frac{\gamma_s}{v(E)} \right) \psi(\vec{r},E,\vec{\Omega},t_s) > . \end{aligned} \quad (17)$$

Hence, by tallying the time-dependent loss term, the denominator of Eq. (9) can be obtained.

2.3 PK Sampling for Uncertainty Assessment

To properly assess the uncertainty of PCQS-MC calculation result, it is imperative to reflect the uncertainty of tallied PK parameters itself. For such a purpose, the PK sampling scheme has been devised and successfully implemented in the iMC code. The basic idea is to capture the stochastic nature of PCQS-MC calculation by sampling the cycle-wise PK corrector power, i.e., for every cycle, the PK equation is solved. However, due to the non-linearity attribute of solving the PK equation, further statistical treatment based on the null hypothesis is often required to harness the proper uncertainty information. Figure 1 illustrates the overall process, and further details can be found in the published work [8].

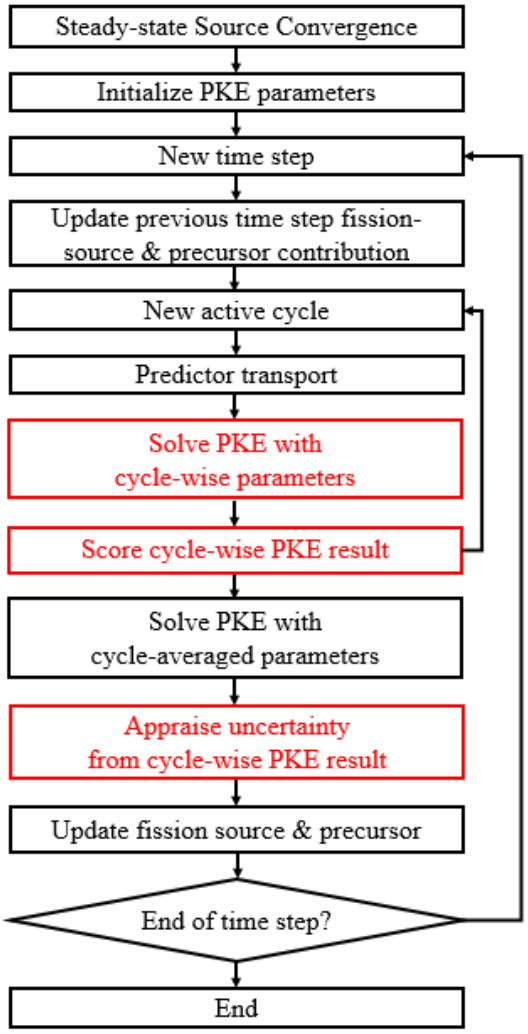

Figure 1. Calculation flow-chart of PCQS-MC including the PK sampling method.

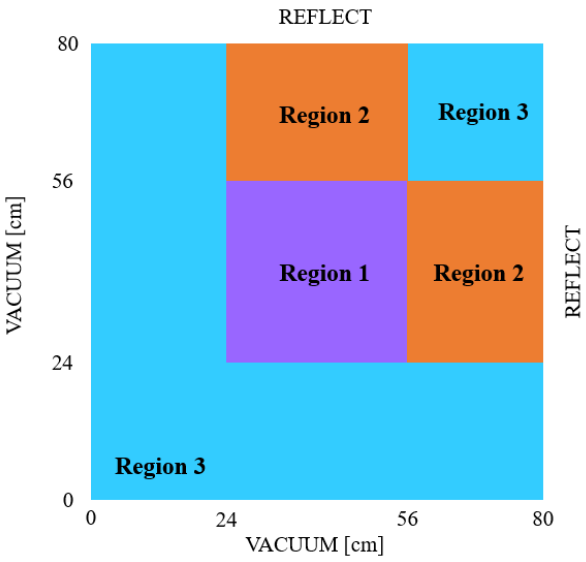

Figure 2. 2-D TWIGL two-group problem layout.

3. Numerical Results

To compare the effect of two different measures for calculating the dynamic reactivity in the PCQS-MC calculation, the well-known TWIGL benchmark has been solved. Figure 2 depicts the problem layout and Figure 3 shows the change in the thermal group cross-section at Region 1 in time to invoke transient. For comparison, both deterministic transport solution based on the Method of Characteristics (MOC) [10] and stochastic transport solution using the DMC approach are shown alongside the PCQS-MC calculation result.

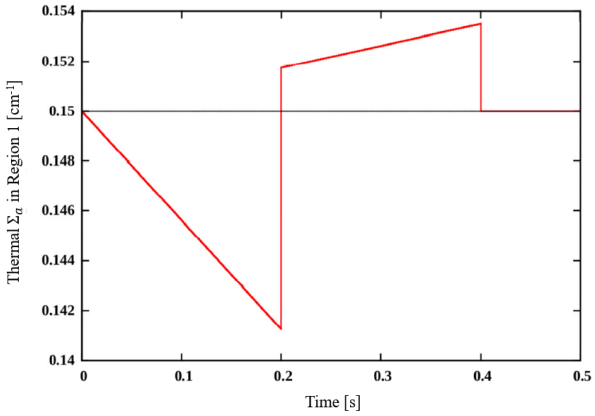

Figure 3. Change in the thermal group absorption cross section at Region 1 in time.

Throughout the discussion, methods 1 and 2 will refer to the direct and indirect calculation approaches respectively, i.e., Eqs. (14) and (15) for method 1 and Eqs. (16) and (17) for method 2. Figures 4 and 5 exhibit the evolution of PCQS-MC calculated power for having 50,000 and 100,000 particles per cycle with a time-step of 0.02 [s]. The number of inactive and active cycles are set to be 100 and 150 for both cases. The error bars denote the 2-sigma uncertainty range estimated from the PK-sampling scheme.

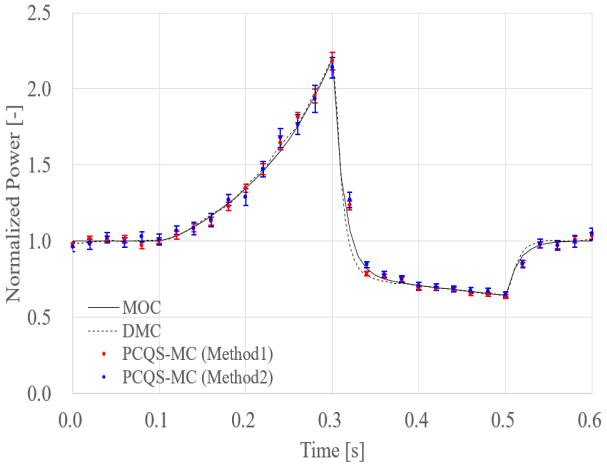

Figure 4. Calculation result with 50,000 particles per cycle (Inactive: 100 / Active: 150).

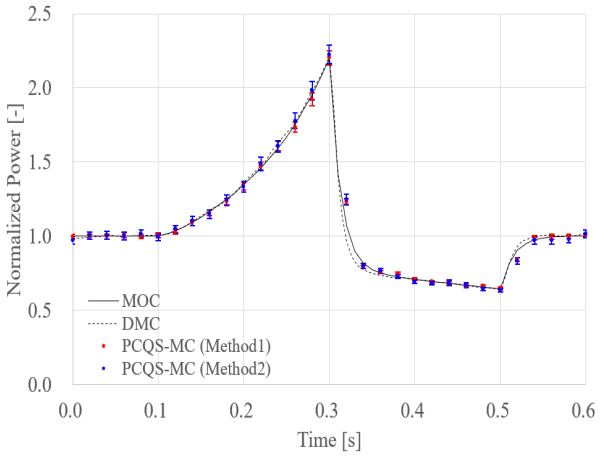

Figure 5. Calculation result with 100,000 particles per cycle (Inactive: 100 / Active: 150).

It could be recognized that all the presented calculation results resemble each other. Nevertheless, it was found that the uncertainty of PCQS-MC calculation based on method 2 always exceeds that of method 1. To further highlight such an innate difference, the cycle-wise PK corrected powers at the peak-time (0.3 s) are compared as shown in Figs. 6 and 7.

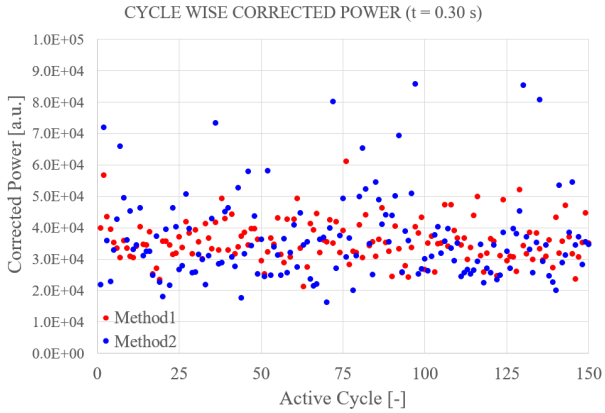

Figure 6. Cycle-wise corrected power at the peak time (Inactive: 100 / Active: 150 / History: 50,000)

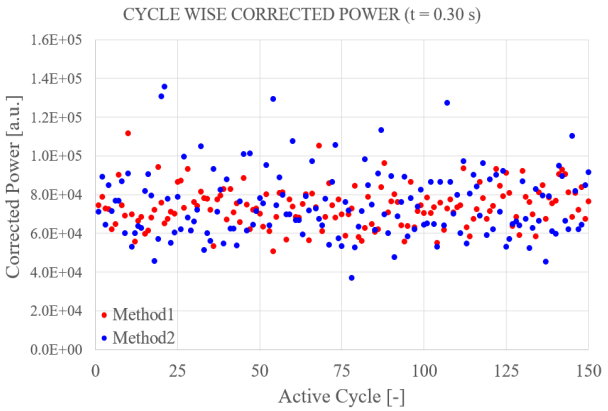

Figure 7. Cycle-wise corrected power at the peak time (Inactive: 100 / Active: 150 / History: 100,000)

4. Conclusions

This work presents the overall description of PCQS-MC transient analysis whilst highlighting different methods for assessing dynamic reactivity. The constituent integral elements can be either directly or indirectly tallied. For having a unit vector weighting, it was found that direct calculation of dynamic reactivity results in a reduced uncertainty, which was assessed using the PK sampling method, for the TWIGL benchmark problem. The cycle-wise corrected power also exhibits consistency, where larger fluctuation was observed for having an indirect assessment of dynamic reactivity.

ACKNOWLEDGEMENTS

This work was supported by the National Research Foundation of Korea Grant funded by the Korean government NRF-2021M2D2A2076383

REFERENCES

[1] M. Faucher, D. Mancusi, and A. Zoia, “New kinetic simulation capabilities for Tripoli-4®: Methods and applications,” Ann. Nucl. Energy, vol. 120, pp. 74–88, 2018.
[2] N. Shaukat, M. Ryu, and H. J. Shim, “Dynamic Monte Carlo transient analysis for the Organization for Economic Co-operation and Development Nuclear Energy Agency (OECD/NEA) C5G7-TD benchmark,” Nucl. Eng. Technol., vol. 49, no. 5, pp. 920–927, 2017.
[3] J. Leppänen, “Development of a dynamic simulation mode in Serpent 2 Monte Carlo code,” Proc. M&C, pp. 5–9, 2013.
[4] A. G. Mylonakis, M. Varvayanni, D. G. E. Grigoriadis, and N. Catsaros, “Developing and investigating a pure Monte-Carlo module for transient neutron transport analysis,” Ann. Nucl. Energy, vol. 104, pp. 103–112, 2017.
[5] Y. Jo, B. Cho, N. Z. Cho, 2016. Nuclear Reactor Transient Analysis by Continuous-Energy Monte Carlo Calculation Based on Predictor-Corrector Quasi-Static Method. Nucl. Sci. Eng., vol. 183, no. 2, pp. 229–246.
[6] X. Guo, X. Shang, J. Song, G. Shi, S. Huang, K. Wang, 2021. Kinetic methods in Monte Carlo code RMC and its implementation to C5G7-TD benchmark. Ann. Nucl. Energy, vol. 151, 107864.
[7] H. Kim, Y. Kim, 2021. A Comparison of Time-Dependent Monte Carlo Frameworks: Predictor-Corrector Quasi-Static Method and Dynamic Simulation. Transactions of the Korean Nuclear Society Virtual Spring Meeting, May 13-14.
[8] T.-s. Oh, Y. Kim, 2023. A new approach for uncertainty quantification in predictor-corrector quasi-static Monte Carlo transient simulation. Front. Energy Res. 11:1089340.
[9] X. Shang, K. Wang, Q. Xu, 2018. Pseudo mesh for adjoint weight flux in predictor corrector quasi static kinetics calculation in Monte Carlo code RMC, Proceedings of Physor 2018, Cancun, Mexico.
[10] B. Cho, N.Z. Cho, Non-overlapping Local/Global (NLG) Iteration Scheme for 2D Transient Method of Characteristics (MOC). Transactions of the Korean Nuclear Society, Spring Meeting, Jeju, May 29-30, 2014.